

Inflammatory Cancer-associated Fibroblast-derived Fibronectin Promotes Oxaliplatin Resistance in Pancreatic Ductal Adenocarcinoma through Integrin-mediated Signaling

Zhaohui Chen^{1,*}, Junfeng Li², Jiexiao Long²

¹*Guangdong Provincial Key Laboratory of Malignant Tumor Pathogenesis and Precision Diagnosis and Treatment, Shenshan Medical Center, Sun Yat-sen Memorial Hospital, Sun Yat-sen University, Shanwei, Guangdong, China*

²*Department of Neurosurgery, Shenshan Medical Center, Sun Yat-sen Memorial Hospital, Sun Yat-sen University, Shanwei, Guangdong, China*

**Corresponding author: chenchh79@mail.sysu.edu.cn*

Keywords: Pancreatic ductal adenocarcinoma, iCAFs, fibronectin, oxaliplatin resistance, ITGA3, bioinformatic analysis

Abstract: Pancreatic ductal adenocarcinoma (PDAC) is characterized by a dense fibrotic stroma. Inflammatory cancer-associated fibroblasts (iCAFs) within this stroma have been implicated in tumor progression, but their role in oxaliplatin resistance remains poorly defined. Here, we isolated iCAFs from oxaliplatin-resistant tumors and identified fibronectin (FN1) as a highly upregulated secretory factor through RNA sequencing. Recombinant FN1 and iCAF-conditioned medium significantly attenuated oxaliplatin-induced cytotoxicity in Panc-1 and MIAPaCa-2 cells, while an anti-FN1 neutralizing antibody reversed the protective effect. Bioinformatic analysis of the GSE79669 dataset revealed elevated FN1 and ITGA3 expression in oxaliplatin-resistant pancreatic cancer cells, and high ITGA3 expression was associated with worse overall and disease-free survival in the TCGA cohort. Pathway enrichment analysis of FN1/ITGA3-coexpressed genes identified focal adhesion, ECM-receptor interaction, PI3K-Akt signaling, regulation of actin cytoskeleton, Rap1 signaling, and Hippo signaling as potentially involved downstream pathways. A protein-protein interaction network further highlighted key nodes within these pathways. These findings demonstrate that iCAF-derived FN1 promotes oxaliplatin resistance in vitro and suggest that ITGA3 integrin signaling may mediate this effect, providing a foundation for future therapeutic targeting of stromal-tumor interactions in pancreatic cancer.

1. Introduction

Pancreatic ductal adenocarcinoma (PDAC) remains one of the most lethal malignancies, with a five-year survival rate below 10% [1,2]. Over 80% of patients present with unresectable disease, and systemic chemotherapy remains the standard of care [3]. Combination regimens including

FOLFIRINOX have improved survival, yet drug resistance ultimately limits their long-term effectiveness [4,5]. Oxaliplatin, a platinum analogue forming DNA crosslinks, is a key component of FOLFIRINOX [6]. Resistance mechanisms involve altered drug transport, enhanced DNA repair, and contributions from the tumor microenvironment [7,8].

The PDAC microenvironment is characterized by dense fibrotic stroma, which may constitute up to 90% of tumor volume [9]. Cancer-associated fibroblasts (CAFs) are the major stromal cells and are now known to comprise functionally distinct subtypes [10,11]. Myofibroblastic CAFs (myCAFs) express high α -smooth muscle actin and reside near neoplastic cells. iCAFs express lower α -SMA but secrete high levels of cytokines, including interleukin-6 [12,13]. A third population, antigen-presenting CAFs (apCAFs), expresses MHC class II molecules [13].

Evidence suggests iCAFs may influence therapeutic response through their secretory activity [14]. For instance, iCAF-derived factors can activate pro-survival pathways. However, the specific contribution of iCAFs to oxaliplatin resistance has not been fully defined.

Fibronectin (FN1) is a large extracellular matrix glycoprotein that interacts with integrin receptors to regulate cell adhesion and signal transduction [15]. Elevated FN1 expression in tumor stroma correlates with poor prognosis in several cancers, including PDAC [16]. In colorectal cancer, FN1 was shown to promote drug resistance through YAP-dependent signaling [17]. In non-small cell lung cancer, FN1 knockdown increased cisplatin sensitivity [18]. These observations suggest CAF-derived FN1 might influence chemosensitivity in PDAC.

In the present study, we isolated iCAFs from oxaliplatin-resistant PDAC tissues and found they secrete high levels of FN1. We tested whether FN1 could directly affect oxaliplatin sensitivity and explored potential receptors and downstream pathways using public transcriptomic datasets.

2. Materials and Methods

2.1 Cell culture

Human PDAC cell lines PANC-1 and MIAPaCa-2 were obtained from the American Type Culture Collection (ATCC, Manassas, VA, USA) and maintained in DMEM supplemented with 10% fetal bovine serum and penicillin/streptomycin at 37°C in 5% CO₂. Normal fibroblasts (NFs) were isolated from non-tumorous pancreatic tissue adjacent to resected tumors. CAFs and iCAFs were isolated from PDAC tissues as described below.

2.2 Isolation of primary fibroblasts

All animal experiments were approved by the Animal Ethical and Welfare Committee of Sun Yat-sen Memorial Hospital, Sun Yat-sen University (Approval No. BAP20240835). Female BALB/c nude mice (5-6 weeks old) were used to establish subcutaneous PDAC xenograft tumors. Oxaliplatin resistance was induced by repeated intraperitoneal administration of oxaliplatin (5 mg/kg) twice weekly for four weeks. Resistant tumors were harvested, minced into 1-2 mm³ and digested with collagenase type I (2 mg/mL), hyaluronidase (1 mg/mL), and DNase I (0.1 mg/mL) for 90 min at 37 °C with gentle agitation. Cell suspensions were filtered through 70- μ m cell strainers and plated in DMEM/F12 medium containing 10% FBS. Adherent fibroblasts were characterized by flow cytometry for PDPN, CD90, and EpCAM to confirm purity (>95% PDPN⁺/CD90⁺/EpCAM⁻). iCAFs were enriched by magnetic-activated cell sorting using an anti-IL-6 antibody (Miltenyi Biotec, Bergisch Gladbach, Germany).

2.3 Immunofluorescence

Cells on glass coverslips were fixed with 4% paraformaldehyde, permeabilized with 0.1% Triton X-100, and blocked with 5% BSA. Primary antibodies against α -SMA (1:200, Abcam) and IL-6 (1:100, Abcam) were applied overnight at 4 °C. Alexa Fluor-conjugated secondary antibodies (Invitrogen) were used for detection. Nuclei were stained with DAPI. Images were acquired on a Leica TCS SP8 confocal microscope.

2.4 RNA sequencing and analysis

Total RNA from NFs, CAFs, and iCAFs was extracted using the RNeasy Mini Kit (Qiagen). Library preparation and sequencing were performed on an Illumina NovaSeq 6000 platform. Reads were aligned to GRCh38 using HISAT2, and differential expression was analyzed with DESeq2 in R. Genes with adjusted $p < 0.05$ and $|\log_2 \text{fold change}| > 1$ were considered significant.

2.5 Quantitative real-time PCR

cDNA was synthesized with the PrimeScript RT Reagent Kit (Takara). qRT-PCR was performed using TB Green Premix Ex Taq II (Takara) on a QuantStudio 6 Flex system. Relative expression was calculated by the $2^{-\Delta\Delta Ct}$ method using GAPDH as reference. Primer sequences are listed in Table 1.

Table 1. Primer sequences for qRT-PCR.

Gene	Forward (5'→3')	Reverse (5'→3')
FN1	ACCTACGGATGACTCGTGCTTT	GCTGTTGTCCTGTGTTGTGGAA
ACTA2	CTATGAGGGCTATGCCTTGCC	GCTCAGCAGTAGTAACGAAGGA
IL6	AGACAGCCACTCACCTCTTCAG	TTCTGCCAGTGCCTCTTTGCTG
GAPDH	GTCTCCTCTGACTTCAACAGCG	ACCACCCTGTTGCTGTAGCCAA

2.6 Enzyme-linked immunosorbent assay

Conditioned medium was collected after 48 h of serum-free culture and concentrated using Amicon Ultra-15 filters with a 10-kDa cutoff (Millipore). FN1 concentration was measured using the Human Fibronectin ELISA Kit (Abcam, ab219046).

2.7 Cell viability and colony formation assays

For viability assays, cells were seeded in 96-well plates and treated with oxaliplatin (0-200 μM) for 48 h in the presence or absence of recombinant FN1 (R&D Systems), iCAF-conditioned medium (CM) (50% v/v), or anti-FN1 neutralizing antibody (10 $\mu\text{g}/\text{mL}$, Santa Cruz). CCK-8 reagent (Dojindo) was added, and absorbance was measured at 450 nm. For colony formation, 1000 cells were plated per well in 6-well plates, treated as indicated, and cultured for 14 days. Colonies were fixed with methanol, stained with 0.5% crystal violet, and manually counted.

2.8 Bioinformatic analyses

The GSE79669 dataset was obtained from GEO, and TCGA-PAAD clinical and expression data were downloaded from the TCGA portal. The GSE79669 dataset contains 14 pancreatic cell lines (7 sensitive, 7 resistant). Gene expression was compared between groups using Student's t-test. Differentially expressed genes between resistant and sensitive cells were identified ($|\log_2 \text{FC}| > 1$,

adjusted $p < 0.05$). Overall survival and disease-free survival were analyzed using the Kaplan-Meier method with log-rank test. Genes co-expressed with both FN1 and ITGA3 in the TCGA-PAAD cohort (Spearman $r > 0.4$, $p < 0.05$) were submitted to KEGG pathway and Gene Ontology enrichment analyses using clusterProfiler. A protein-protein interaction network was constructed using the STRING database (version 11.5) and visualized in Cytoscape.

2.9 Statistical analysis

Data are presented as mean \pm SD from at least three independent experiments. Comparisons between two groups used Student's t-test. Multiple group comparisons used one-way ANOVA with Tukey's post hoc test. $p < 0.05$ was considered statistically significant.

3. Results

3.1 iCAFs from oxaliplatin-resistant PDAC exhibit low α -SMA and high IL-6 expression

We first characterized fibroblasts isolated from oxaliplatin-resistant tumors and compared them with normal fibroblasts. Immunofluorescence staining showed that NFs were positive for α -SMA and weakly positive for IL-6. CAFs showed enhanced staining for both markers. iCAFs displayed significantly weaker α -SMA but stronger IL-6 immunofluorescence compared with NFs and CAFs (Figure 1A). Quantification confirmed these differences in fluorescence intensity (Figure 1B-C). Phase-contrast images showed that NFs appeared as elongated spindle cells, CAFs were more stellate, and iCAFs were rounded with granular cytoplasm (Figure 1D). These findings indicate that iCAFs from oxaliplatin-resistant tumors possess a distinct morphology and higher proliferative capacity than CAFs.

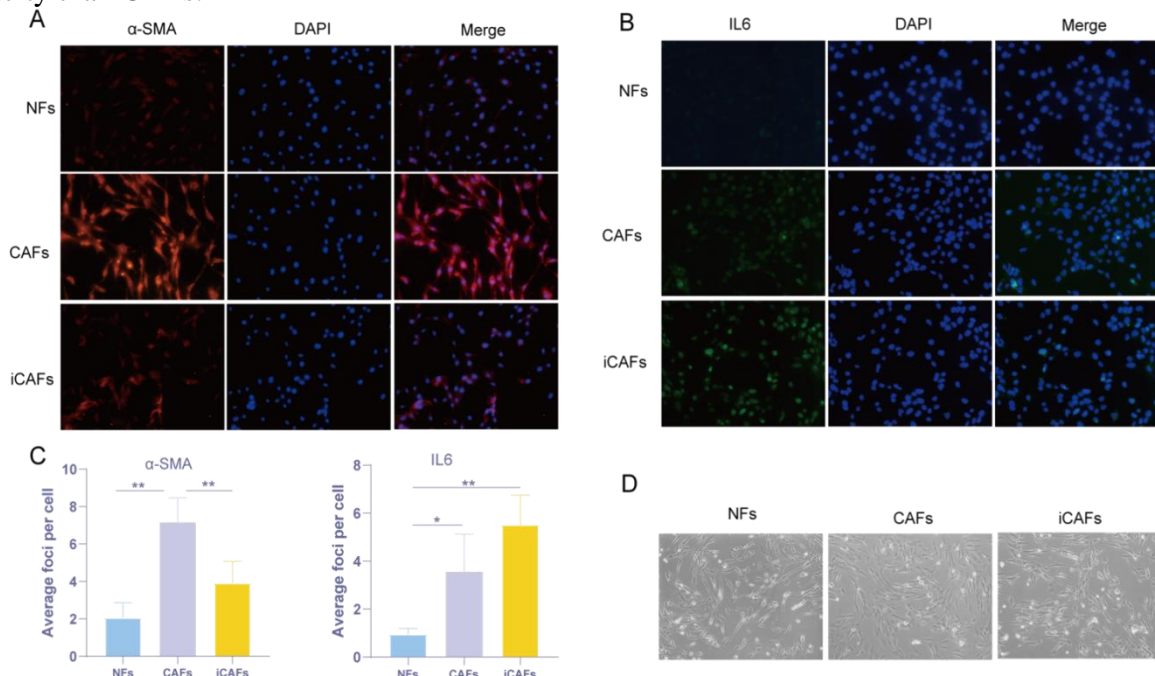


Figure 1. Characterization of iCAFs from oxaliplatin-resistant PDAC. (A) Immunofluorescence for α -SMA (green) and IL-6 (red) in NFs, CAFs, and iCAFs. Nuclei stained with DAPI (blue). Scale bar = 50 μ m. (B-C) Quantification of α -SMA and IL-6 fluorescence intensity. (D) Phase-contrast images showing cell morphology.

3.2 FN1 is highly expressed in iCAFs and mediates oxaliplatin resistance

To identify secreted factors that might contribute to resistance, we performed RNA-seq on NFs, CAFs, and iCAFs. FN1 was among the most upregulated transcripts in iCAFs compared with NFs and CAFs. qRT-PCR confirmed that FN1 mRNA was significantly elevated in iCAFs relative to NFs (Figure 2A). ELISA showed markedly higher FN1 protein concentrations in iCAF-conditioned medium compared to NFs (Figure 2B).

We then asked whether FN1 could directly modulate oxaliplatin sensitivity. PANC-1 cells were cultured with recombinant FN1 or conditioned medium from different fibroblast types and exposed to oxaliplatin. Colony formation assays showed that oxaliplatin treatment reduced colony numbers compared to untreated cells. NFs-CM did not rescue colony formation, whereas CAFs-CM partially restored clonogenic growth. iCAFs-CM significantly increased colony numbers compared to oxaliplatin alone, and recombinant FN1 produced a similar protective effect (Figure 2C-D). These findings indicate that iCAF-secreted FN1 is a key mediator of oxaliplatin resistance in vitro.

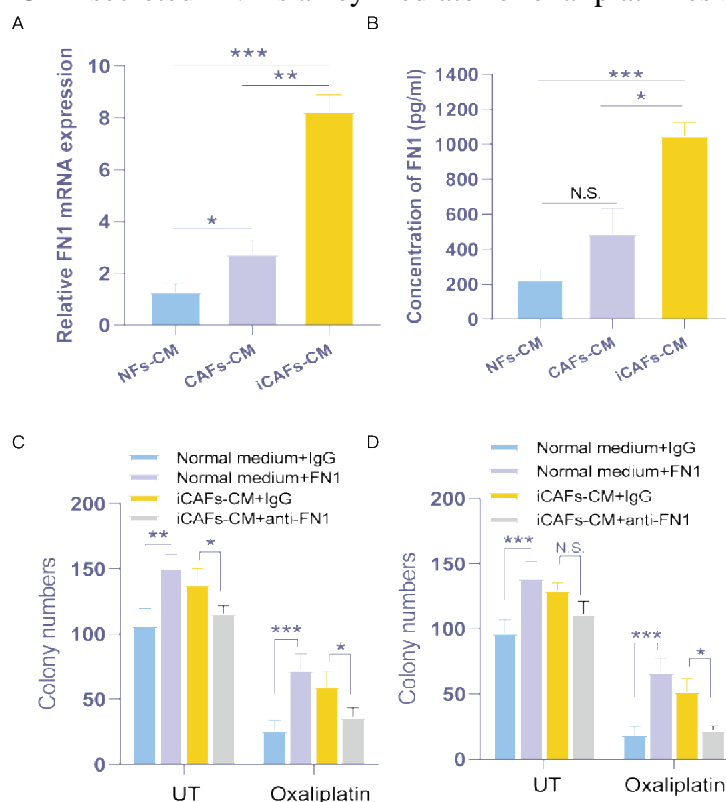


Figure 2. iCAF-secreted FN1 promotes oxaliplatin resistance in vitro. (A) Relative FN1 mRNA expression in NFs, CAFs, and iCAFs measured by qRT-PCR. (B) FN1 concentrations in conditioned medium measured by ELISA. (C-D) Colony formation assays under the indicated treatments. UT, untreated; Oxa, oxaliplatin; rhFN1, recombinant human FN1.

3.3 Bioinformatic analyses of FN1 and ITGA3 in oxaliplatin-resistant pancreatic cancer

To explore the potential integrin receptor for FN1, we analyzed the GSE79669 dataset containing 14 pancreatic cell lines (7 oxaliplatin-sensitive, 7 oxaliplatin-resistant). The volcano plot illustrated the distribution of differentially expressed genes between the two groups, with ITGA3 highlighted among the upregulated genes (Figure 3A). A positive correlation was observed between FN1 and ITGA3 expression (Figure 3B). Boxplots showed that FN1 was significantly higher in

oxaliplatin-resistant cells than in sensitive cells, while ITGA3 exhibited a similar but non-significant trend (Figure 3C-D). Differential gene expression analysis also identified ITGA3 among the upregulated genes in resistant cells. Kaplan-Meier survival analysis of TCGA-PAAD patients stratified by ITGA3 expression showed that high ITGA3 expression was significantly associated with both worse overall survival (log-rank $p = 0.0002$, HR = 1.8) and worse disease-free survival (log-rank $p = 0.0002$, HR = 1.3) (Figure 3E-F). These results support ITGA3 as a candidate receptor for FN1 and suggest its potential clinical relevance.

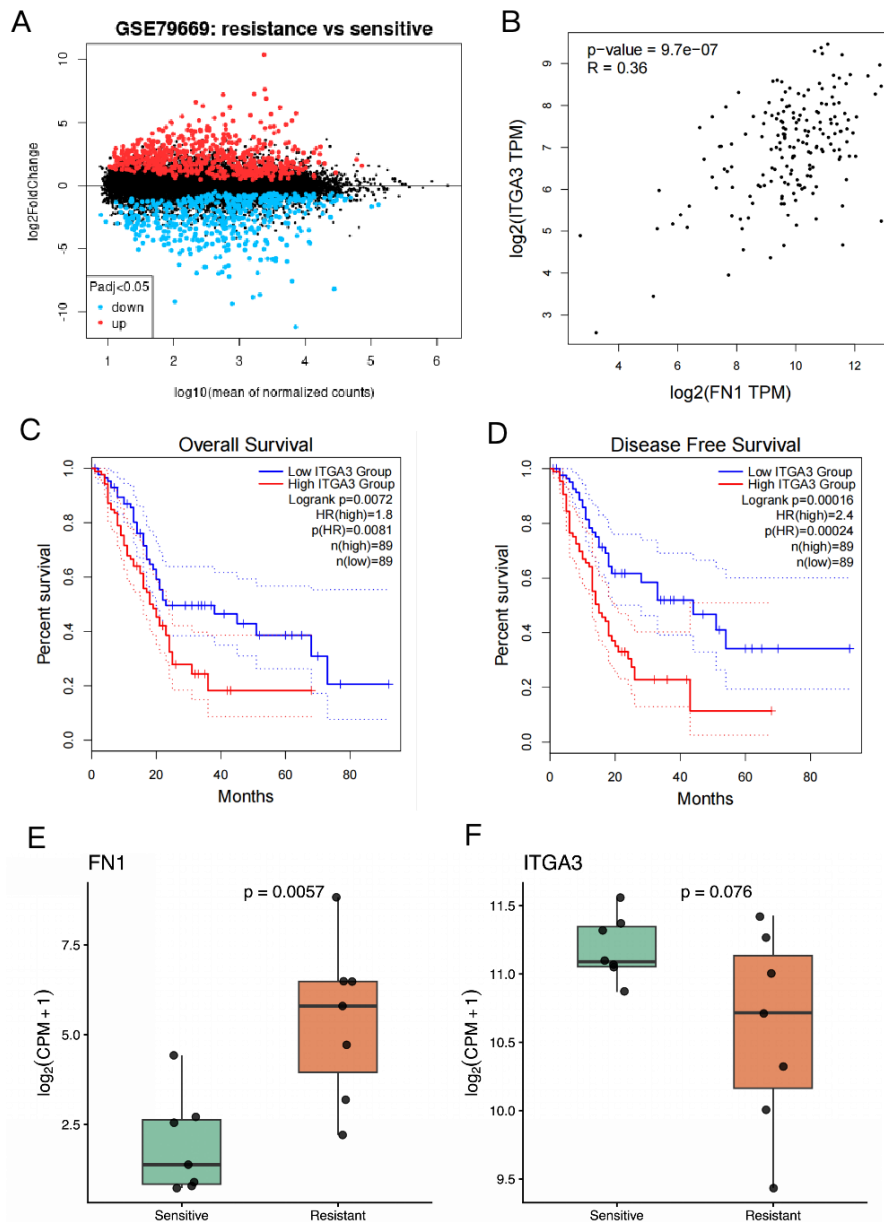


Figure 3. Bioinformatic analysis of FN1 and ITGA3 expression in GSE79669 and TCGA. (A) Volcano plot of differentially expressed genes in GSE79669; ITGA3 is among the upregulated genes. (B) Positive correlation between FN1 and ITGA3 expression. (C) Boxplot showing FN1 expression in sensitive (n=7) vs. resistant (n=7) cell lines. (D) Boxplot showing ITGA3 expression. (E) Overall survival of TCGA-PAAD patients stratified by ITGA3 expression. (F) Disease-free survival stratified by ITGA3 expression.

3.4 Pathway enrichment and protein interaction network

To identify downstream pathways potentially activated by the FN1-ITGA3 axis, we analyzed 15 genes co-expressed with both FN1 and ITGA3 in the TCGA-PAAD cohort (Figure 4A). Gene Ontology biological process analysis showed enrichment for terms related to cell adhesion and extracellular matrix organization (Figure 4B). KEGG pathway enrichment analysis identified six significantly enriched pathways: focal adhesion, ECM-receptor interaction, PI3K-Akt signaling, regulation of actin cytoskeleton, Rap1 signaling, and Hippo signaling (Figure 4C). Protein-protein interaction network analysis constructed from these genes revealed a connected network with several central nodes (Figure 4D). These findings suggest that multiple integrin-related signaling cascades, including focal adhesion and Hippo pathways, may be involved in FN1-mediated oxaliplatin resistance.

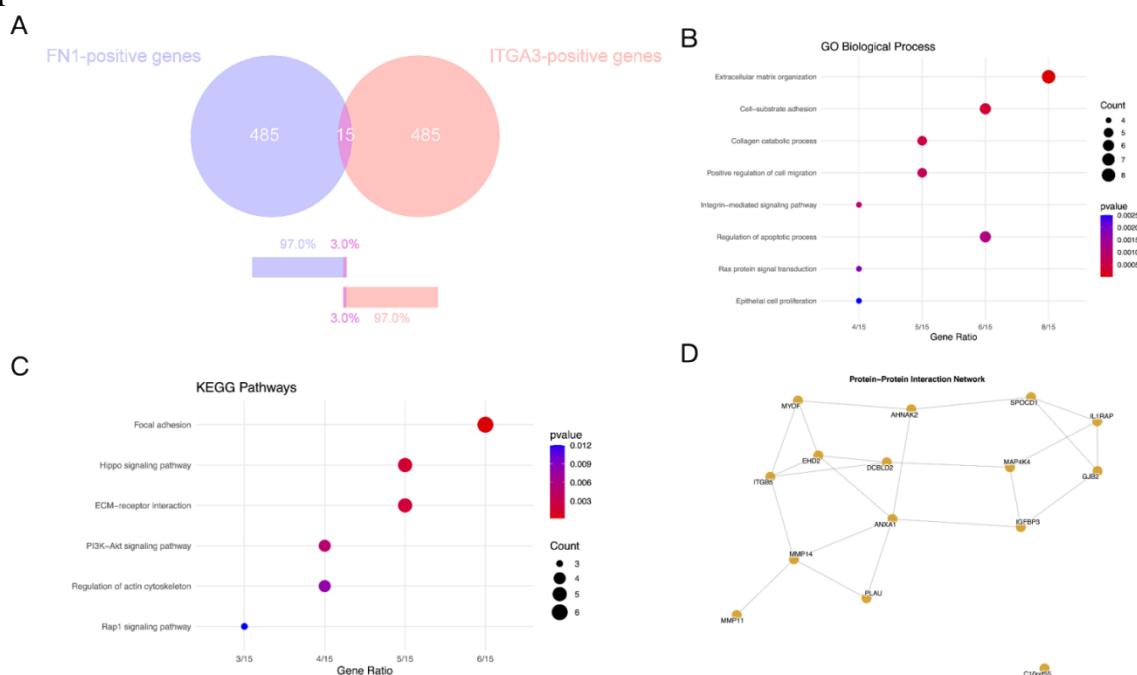


Figure 4. Pathway enrichment and protein interaction network. (A) co-expressed genes in FN1 and ITGA3. (B) Gene Ontology biological process enrichment. (C) KEGG pathway enrichment of FN1/ITGA3 co-expressed genes. (D) Protein-protein interaction network constructed with STRING.

4. Discussion

In this study, we demonstrated that iCAFs isolated from oxaliplatin-resistant PDAC tissues secrete high levels of fibronectin, and that this FN1 protects PDAC cells from oxaliplatin-induced cytotoxicity. Analysis of public datasets identified ITGA3 as a candidate receptor and highlighted several integrin-related pathways that may mediate the downstream effects.

CAF heterogeneity has become increasingly recognized in recent years [10,11]. Single-cell analyses have shown that iCAFs, myCAFs, and apCAFs represent transcriptionally distinct populations with different functions [12,13]. Our observation that iCAFs predominate in oxaliplatin-resistant tissues is consistent with a report that CAFs from platinum-resistant PDAC patients exhibit iCAF-like features [19]. The increased proliferative capacity of iCAFs compared to CAFs in our study further supports their functional distinctiveness.

FN1 has been implicated in drug resistance across multiple cancer types. In colorectal cancer, FN1 promotes drug resistance through YAP-dependent signaling [17]. In lung cancer, FN1

silencing increases cisplatin sensitivity [18]. In PDAC, stromal FN1 expression has been proposed as a prognostic marker [16], and macrophage-derived FN1 was shown to affect gemcitabine response [20]. Our findings extend this work by identifying iCAFs as a major source of FN1 in the oxaliplatin-resistant microenvironment and demonstrating that iCAF-derived FN1 directly reduces oxaliplatin sensitivity.

The bioinformatic analyses provide mechanistic clues. Our analysis of the GSE79669 dataset indicated a tendency toward higher ITGA3 expression in oxaliplatin-resistant cells, although the difference did not reach statistical significance. The association of high ITGA3 expression with worse overall and disease-free survival in TCGA-PAAD patients further supports its clinical relevance. ITGA3 was previously reported as a biomarker in PDAC [21]. In other systems, ITGA3 engagement has been linked to FAK activation and YAP nuclear translocation [22].

The pathway enrichment analysis identified focal adhesion, ECM-receptor interaction, PI3K-Akt, regulation of actin cytoskeleton, Rap1 signaling, and Hippo signaling as potentially involved pathways. These findings are consistent with the known role of integrins in mediating cell-matrix interactions and activating multiple downstream signaling cascades that regulate cell survival, proliferation, and drug resistance.

Several limitations should be acknowledged. First, evidence for ITGA3 as the functional receptor and for the identified pathways is based on bioinformatic correlation rather than direct experimental validation. Functional experiments are needed to establish causality. Second, *in vivo* experiments were not performed, limiting translational relevance. Third, we focused only on oxaliplatin; whether the same mechanism applies to other agents remains unknown. Fourth, other iCAF-derived factors may contribute to chemoresistance. Despite these limitations, our findings point to potential therapeutic opportunities. Disrupting the FN1-ITGA3 interaction or inhibiting downstream pathways could enhance oxaliplatin efficacy. Several FAK inhibitors are in clinical development [23], and agents targeting the Hippo pathway are emerging [24].

In conclusion, this study provides *in vitro* evidence that iCAF-derived FN1 promotes oxaliplatin resistance in PDAC. Bioinformatic analyses implicate ITGA3 as a candidate receptor and identify multiple integrin-related pathways that may mediate downstream effects. These findings establish a basis for subsequent experimental and translational investigations.

5. Conclusions

iCAFs isolated from oxaliplatin-resistant PDAC secrete high levels of fibronectin, which directly reduces oxaliplatin sensitivity in PDAC cells *in vitro*. The GSE79669 dataset shows that both FN1 and ITGA3 are upregulated in oxaliplatin-resistant cells. High ITGA3 expression is associated with worse survival in TCGA-PAAD patients. Pathway analysis of FN1/ITGA3 co-expressed genes identifies focal adhesion, ECM-receptor interaction, PI3K-Akt, actin cytoskeleton regulation, Rap1, and Hippo signaling as potentially involved pathways. Experimental validation is warranted.

Abbreviations

ANOVA, analysis of variance; CAF, cancer-associated fibroblast; CCK-8, Cell Counting Kit-8; CM, conditioned medium; DAPI, 4',6-diamidino-2-phenylindole; DMEM, Dulbecco's Modified Eagle Medium; ECM, extracellular matrix; ELISA, enzyme-linked immunosorbent assay; FAK, focal adhesion kinase; FBS, fetal bovine serum; FN1, fibronectin 1; GO, Gene Ontology; iCAF, inflammatory cancer-associated fibroblast; IL-6, interleukin-6; ITGA3, integrin subunit alpha 3; KEGG, Kyoto Encyclopedia of Genes and Genomes; NF, normal fibroblast; PBS, phosphate-buffered saline; PDAC, pancreatic ductal adenocarcinoma; PPI, protein-protein interaction; qRT-PCR, quantitative real-time polymerase chain reaction; RNA-seq, RNA sequencing; SD, standard

deviation; TCGA, The Cancer Genome Atlas; YAP, Yes-associated protein; α -SMA, alpha-smooth muscle actin.

Authors' contributions

Zhaohui Chen conceived the study, performed experiments, analyzed data, and drafted the manuscript. Junfeng Li performed cell culture and viability assays. Jiexiao Long contributed to data analysis and figure preparation. All authors read and approved the final manuscript.

Availability of data and materials

The RNA-seq data are available from the corresponding author upon reasonable request. Public datasets analyzed in this study are available from TCGA (<https://portal.gdc.cancer.gov>) and GEO (accession GSE79669).

Acknowledgement

This work was supported by the Shanwei Municipal Science and Technology Plan Project (Grant No.2024C041) and Guangdong Science and Technology Department (Grant No. 2024B1212030002).

References

- [1] Siegel RL, Miller KD, Fuchs HE, Jemal A. *Cancer statistics, 2022*. *CA Cancer J Clin*. 2022;72(1):7-33. doi:10.3322/caac.21708.
- [2] Rahib L, Smith BD, Aizenberg R, Rosenzweig AB, Fleshman JM, Matrisian LM. *Projecting cancer incidence and deaths to 2030: the unexpected burden of thyroid, liver, and pancreas cancers in the United States*. *Cancer Res*. 2014;74(11):2913-2921. doi:10.1158/0008-5472.CAN-14-0155.
- [3] Park W, Chawla A, O'Reilly EM. *Pancreatic cancer: a review*. *JAMA*. 2021;326(9):851-862. doi:10.1001/jama.2021.13027.
- [4] Conroy T, Desseigne F, Ychou M, et al. *FOLFIRINOX versus gemcitabine for metastatic pancreatic cancer*. *N Engl J Med*. 2011;364(19):1817-1825. doi:10.1056/NEJMoa1011923.
- [5] Von Hoff DD, Ervin T, Arena FP, et al. *Increased survival in pancreatic cancer with nab-paclitaxel plus gemcitabine*. *N Engl J Med*. 2013;369(18):1691-1703. doi:10.1056/NEJMoa1304369.
- [6] Raymond E, Faivre S, Chaney S, Woynarowski J, Cvitkovic E. *Cellular and molecular pharmacology of oxaliplatin*. *Mol Cancer Ther*. 2002;1(3):227-235.
- [7] Yu S, Zhang C, Xie KP. *Therapeutic resistance of pancreatic cancer: roadmap to its reversal*. *Biochim Biophys Acta Rev Cancer*. 2021;1875(1):188461. doi:10.1016/j.bbcan.2020.188461.
- [8] Nevala-Plagemann C, Hidalgo M, Garrido-Laguna I. *From state-of-the-art treatments to novel therapies for advanced-stage pancreatic cancer*. *Nat Rev Clin Oncol*. 2020;17(2):108-123. doi:10.1038/s41571-019-0281-6.
- [9] Whatcott CJ, Diep CH, Jiang P, et al. *Desmoplasia in primary tumors and metastatic lesions of pancreatic cancer*. *Clin Cancer Res*. 2015;21(15):3561-3568. doi:10.1158/1078-0432.CCR-14-1051.
- [10] Sahai E, Astsaturov I, Cukierman E, et al. *A framework for advancing our understanding of cancer-associated fibroblasts*. *Nat Rev Cancer*. 2020;20(3):174-186. doi:10.1038/s41568-019-0238-1.
- [11] Biffi G, Tuveson DA. *Diversity and biology of cancer-associated fibroblasts*. *Physiol Rev*. 2021;101(1):147-176. doi:10.1152/physrev.00048.2019.
- [12] Öhlund D, Handly-Santana A, Biffi G, et al. *Distinct populations of inflammatory fibroblasts and myofibroblasts in pancreatic cancer*. *J Exp Med*. 2017;214(3):579-596. doi:10.1084/jem.20162024.
- [13] Elyada E, Bolisetty M, Laise P, et al. *Cross-species single-cell analysis of pancreatic ductal adenocarcinoma reveals antigen-presenting cancer-associated fibroblasts*. *Cancer Discov*. 2019;9(8):1102-1123. doi:10.1158/2159-8290.CD-19-0094.
- [14] Boyd LNC, Andini KD, Peters GJ, Kazemier G, Giovannetti E. *Heterogeneity and plasticity of cancer-associated fibroblasts in the pancreatic tumor microenvironment*. *Semin Cancer Biol*. 2022;82:184-196. doi:10.1016/j.semcancer.2021.03.006.
- [15] Pankov R, Yamada KM. *Fibronectin at a glance*. *J Cell Sci*. 2002;115(Pt 20):3861-3863. doi:10.1242/jcs.00059.

- [16] Hiroshima Y, Kasajima R, Kimura Y, Komura D, Miyagi Y. Novel targets identified by integrated cancer-stromal interactome analysis of pancreatic adenocarcinoma. *Cancer Lett.* 2020;469:217-227. doi:10.1016/j.canlet.2019.10.031.
- [17] Ye Y, Zhang R, Feng H. Fibronectin promotes tumor cells growth and drugs resistance through a CDC42-YAP dependent signaling pathway in colorectal cancer. *Cell Biol Int.* 2020;44(9):1840-1849. doi:10.1002/cbin.11390.
- [18] Gao W, Liu Y, Qin R, Liu D, Feng Q. Silence of fibronectin 1 increases cisplatin sensitivity of non-small cell lung cancer cell line. *Biochem Biophys Res Commun.* 2016;476(1):35-41. doi:10.1016/j.bbrc.2016.05.081.
- [19] Zhang X, Zheng S, Hu C, et al. Cancer-associated fibroblast-induced lncRNA UPK1A-AS1 confers platinum resistance in pancreatic cancer via efficient double-strand break repair. *Oncogene.* 2022;41(16):2372-2389. doi:10.1038/s41388-022-02265-4.
- [20] Xavier CPR, Castro I, Caires HR, et al. Chitinase 3-like-1 and fibronectin in the cargo of extracellular vesicles shed by human macrophages influence pancreatic cancer cellular response to gemcitabine. *Cancer Lett.* 2021;501:210-223. doi:10.1016/j.canlet.2020.11.013.
- [21] Lei X, Li Y, Chen Z, et al. Comprehensive analysis of abnormal expression, prognostic value and oncogenic role of the hub gene FN1 in pancreatic ductal adenocarcinoma via bioinformatic analysis and in vitro experiments. *PeerJ.* 2021;9:e12141. doi:10.7717/peerj.12141.
- [22] Hu JK, Du W, Shelton SJ, Oldham MC, DiPersio CM, Klein OD. An FAK-YAP-mTOR signaling axis regulates stem cell-based tissue renewal in mice. *Cell Stem Cell.* 2017;21(1):91-106. doi:10.1016/j.stem.2017.03.023.
- [23] Lv PC, Jiang AQ, Zhang WM, Zhu HL. FAK inhibitors in cancer, a patent review. *Expert Opin Ther Pat.* 2018;28(2):139-145. doi:10.1080/13543776.2018.1414183.
- [24] Liu-Chittenden Y, Huang B, Shim JS, et al. Genetic and pharmacological disruption of the TEAD-YAP complex suppresses the oncogenic activity of YAP. *Genes Dev.* 2012;26(12):1300-1305. doi:10.1101/gad.192856.112.